

# High-frequency, plane-wave, multi-pulse acoustic contrast agent imaging at 16 MHz

Jeffrey A. Ketterling  
Lizzi Center for Biomedical Engineering  
Riverside Research  
New York, NY

Ronald H. Silverman  
Department of Ophthalmology  
Harkness Eye Institute  
Columbia University Irving Medical Center  
New York, NY

**Abstract**—Multi-pulse (MP) ultrasound contrast agent (UCA) imaging techniques take advantage of the nonlinear response of UCAs by transmitting 2 or more pulses of different phase or amplitude and combining them in such a way as to reduce the linear component of the backscatter (i.e., tissue) and emphasize the nonlinear components (i.e., UCA). The MP methods of pulse inversion (PI, +1 and -1 pair) and amplitude modulation (AM, +1 and +1/2 pair) were compared to standard multi-angle, high-speed plane-wave compound imaging for a flow of the UCA DEFINITY<sup>®</sup> using a Verasonics Vantage 128 and an 18-MHz linear array. Transmissions were made at -10, 1 and 10 degrees. The PI and AM methods used a pulse pair at each angle and standard plane-wave imaging used a single transmission at each angle. DEFINITY<sup>®</sup> was diluted in water to 2000:1 and then a circular flow was established through a 2-mm flow phantom in a tissue mimicking material. Beamformed data were processed to find the RMS values in the flow and depth matched background region in order to calculate a contrast-to-tissue ratio (CTR). MP methods resulted in a 5-10 dB improvement in CTR relative to standard multi-angle plane-wave imaging at 16 MHz.

## I. INTRODUCTION

In order to improve the contrast-to-tissue ratio (CTR), multi-pulse transmission approaches have been employed that take advantage of the nonlinear pressure- or phase-dependent response of ultrasound contrast agents (UCAs) [1]. These approaches transmit a sequence of low and high amplitude waveforms or inverted waveforms [2]. Broadly, the methods are categorized as pulse inversion (PI) [3] or amplitude modulation (AM) [4]. Nonlinear imaging approaches ideally require a transducer with sufficient bandwidth to detect energy at the desired frequencies or a compromise can be made by shifting the transmit towards one edge of the bandwidth. Due to the multi-pulse aspect of many nonlinear imaging approaches, the effective frame rate decreases as the number of transmissions lines increase.

Frame-rate limitations imposed by multi-pulse nonlinear imaging modes can be overcome by using plane-wave approaches [5]–[7]. The unfocused nature of coherent wavefront transmissions reduces peak pressures relative to traditional line-by-line image formation, but nonlinear imaging generally requires lower pressures in order to avoid UCA destruction. UCAs are usually optimized for imaging in the low-MHz frequency range with the peak distribution sized in the 1-3  $\mu\text{m}$  diameter range. However, UCAs have a wide size distribution and some fraction of agents will be smaller and will respond

to frequencies above 10 MHz [8], [9]. These frequencies are of interest for small-animal and small-parts imaging [10]. Multi-pulse, high-speed plane-wave imaging approaches at high-frequencies have, to date, been minimally examined.

Here, we examined the UCA DEFINITY<sup>®</sup> (Lantheus Medical Imaging, Inc., N. Billerica, MA) using an 18-MHz linear array with plane-wave excitation in order to assess the level of tissue suppression relative to the contrast flow using a PI and AM approach.

## II. METHODS

### A. Plane Wave Excitation

Data were acquired with a Vantage 128 (Verasonics, Redmond, WA) and an 18-MHz, 128 element linear array with an 8-mm elevation focus (Verasonics L22-14v). The transducer was attached to an automated 3-axis motion system. Data were acquired at a sampling rate of 62.5 MHz and a 1 to 30 MHz digital bandpass filter was used on receive. The receive signal underwent a depth dependent gain. The raw receive data were post-processed to generate beamformed data [11] that maintained the sampling rate of the original data (62.5 MHz) and 256 RF lines were formed with 50  $\mu\text{m}$  spacing between lines. Three modes were used for imaging: standard multi-angle plane-wave imaging with batches of transmissions sweeping a defined angle range, PI with a +1 and -1 transmission pair at each angle, and AM with a +1 and +1/2 transmission at each angle.

After beamforming, rectangular regions of interest (ROI) were defined within the flow region and at the depth of the flow channel within the background material (0.7 mm x 4.8 mm). The root-mean-square (RMS) of the RF data in the ROI was calculated and absolute magnitudes could be compared or the ratio of flow-to-background provided a CTR. ANOVA and post-hoc Tukey tests (OriginLab 2019, Northampton, MA) were used to determine if significance existed between the CTR values for multi-pulse and standard multi-angle plane wave imaging cases. Significance was defined as  $p < 0.05$ .

### B. Contrast agent

Experiments were performed with the UCA DEFINITY<sup>®</sup>. The agent was prepared as recommended by the manufacturer using an agitator (Vialmix, Lantheus Medical Imaging, Inc., N. Billerica, MA) for a 45-s duration. Size distribution has

been reported to be primarily in the 1 to 3  $\mu\text{m}$  range with  $1.6 \times 10^{10}$  bubbles/ml [12]. Prior to an experiment, 0.1 mL of DEFINITY<sup>®</sup> was diluted into a 200 mL reservoir of filtered water (2000:1 ratio). Data from a total of  $N = 15$  experimental runs were collected. Each experimental run for a collection of standard multi-angle plane wave, PI and AM data took on the order of 5 minutes.

### C. Flow Phantom

A custom, wall-less flow phantom with a 2-mm diameter channel was used to simulate flow in a vessel (CIRS, Norfolk, VA). The top of the channel was situated 2.75 mm below the phantom surface. Speed of sound in the proprietary urethane rubber was 1460 m/s and, at 15 MHz, attenuation was estimated to be 1.8 to 2.5 dB/cm/MHz [13]. This material has a nonlinear relation between attenuation ( $\alpha$ ) and frequency ( $f$ ):  $\alpha = 0.18 * f^{1.83}$  [13]. Before entering the flow channel, the acoustic pressure was, therefore, attenuated by  $\approx 8$  dB at 15 MHz.

A reservoir of diluted UCA was placed on a stir plate and a recirculation flow through the channel was established with a micropump (REGLO-Z Digital ISM901B, Ismatec, Glattbrugg, Switzerland) and suction flow head (GA Series, Micropump, Inc., Vancouver, WA). The phantom was placed at a slight upward tilt in the downstream flow direction to reduce the likelihood of UCA building up at the top surface of the flow channel. A single flow rate of 6 mL/min was used which corresponded to an average flow velocity of 3.2 cm/s. The elevation focus of the linear array (8 mm) was placed at the center of the channel and the flow passed through the image plane in the lateral direction.

### D. Acoustic-field Characterization

The sound field of the array was characterized with a calibrated 40- $\mu\text{m}$  needle hydrophone (Precision Acoustics Ltd., Dorset, UK). An output trigger synchronized to the transmitted plane waves was used to trigger an acquisition on an external digitizer. The waveforms were sampled at 250 MHz. Transmit/receive waveforms were acquired from a 25- $\mu\text{m}$  diameter wire target placed in the center of the linear-array acoustic field at an 8-mm axial distance. The pressure versus drive voltage and sensitivity versus drive frequency were quantified.

## III. RESULTS

### A. Acoustic Field

The peak-negative acoustic pressure as a function of drive voltage, transmission angle and polarity of transmission is shown in Fig. 1 for transmit angles of [-10 1 10] degrees. The positive (+1) transmissions are shown as lines while the inverted (-1) transmissions are shown as symbols with matching color. Only a single location was measured at the center of the transducer at a distance of 8 mm.

Figure 2 shows the raw, non-beamformed, time domain receive waveforms from a 25- $\mu\text{m}$  wire target for AM and PI transmissions with a -10 degree and 10 V (0.84 MPa)

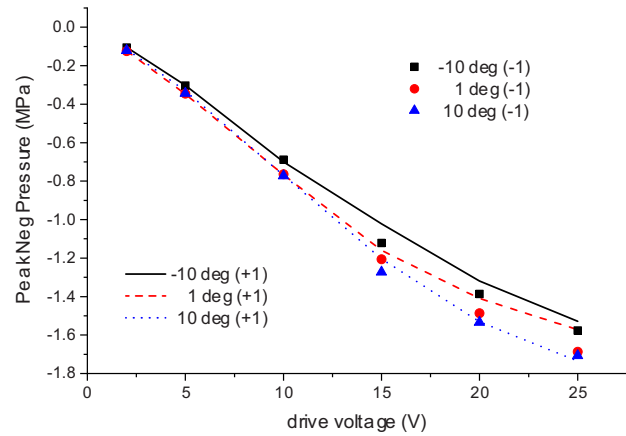


Fig. 1. Peak negative acoustic pressure in water at a distance of 8 mm as a function of drive voltage and transmission angle for a 16 MHz, 1.5 cycle transmission. The +1 cases (lines) represent normal transmission phase and the -1 cases (symbols) are with the waveform inverted.

transmission. The AM waveforms represent 1 (solid) and 1/2 (dashed) amplitude but the 1/2 amplitude was received and displayed with a gain of -2 in order to simplify post-processing. PI waveforms show the +1 (solid) and -1 (dashed) amplitude transmission. The waveform pairs show the inverted phase of transmission. Comparing the +1 cases from the AM and PI transmissions revealed that they were not exact replicates which provides a source for increased residual because of small variations in pulse-to-pulse waveforms. The AM case was also not optimally matched as was seen by the increased residual relative to the PI case.

The transmit/receive frequency response of the array for defined transmission frequencies between 8 and 24 MHz were measured using a 25- $\mu\text{m}$  diameter wire target (Fig. 3, triangles). These data were acquired with a bandpass of 1 to 31 MHz. The peak echo amplitude occurred for a 14-MHz transmit frequency and then decreased on either end of the bandwidth. At 8 and 24 MHz the transmit/receive sensitivity was down by 14 dB from that at 14 MHz. The 6-dB bandwidth center frequencies (squares) are also plotted as a function of transmit frequency. The defined transmit frequency and receive center frequency were close to 1-to-1 from 8 to 14 MHz. Above 14 MHz, the receive frequency began to flatten. At a 24 MHz transmit the receive center frequency was 18 MHz.

### B. Flow Phantom

Figure 4 shows representative B-mode images of the contrast flow for standard multi-angle plane-wave compounding, AM and PI. The standard compound plane wave case with 3 transmissions, [-10 1 10 degrees], had similar image intensities for the flow and background material. The AM case had an increased contrast between the background and the flow, but the change was less pronounced than for the PI case.

The changes in contrast for the standard, 3-angle compound plane-wave, AM and PI cases over the range of acoustic drive pressures are summarized in Fig. 5. The figure contains a second pressure scale bar that accounts for the 2.75 mm of

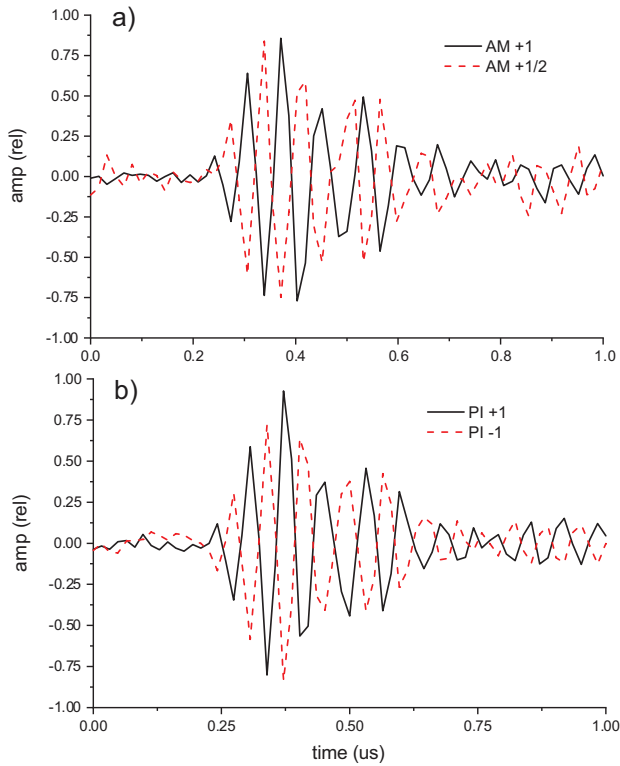


Fig. 2. Raw time-domain waveforms on a central array element from a 25  $\mu\text{m}$  diameter wire target with a 16 MHz, 1.5 cycle, 10 V (0.84 MPa) and -10 degree transmission angle using an a) AM and b) PI scheme. The AM +1/2 waveform was doubled in amplitude and inverted upon receive and displayed as such.

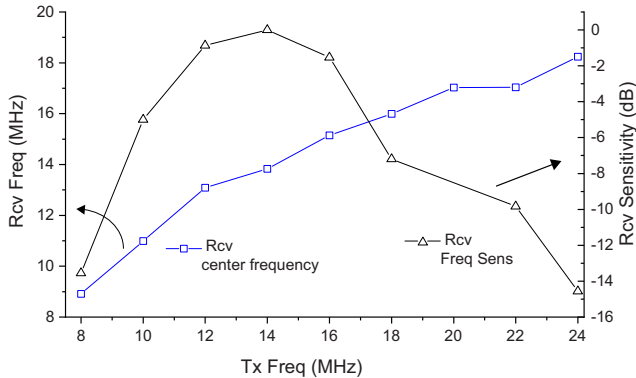


Fig. 3. Peak spectral amplitude (triangles) and -6-dB center frequency (squares) as a function of transmit drive frequency using a 25- $\mu\text{m}$  diameter wire as a point target. The target was placed in the center of the linear array at an 8 mm distance. The transmit waveform was 1.5 cycles with a 2 V (0.13 MPa) transmission.

attenuation in the tissue-mimicking material. The intensity of the background signal was seen to increase with acoustic drive pressure as would be expected (Fig. 5a). The region of flow was visible against the phantom background at all acoustic drive pressures. The PI background intensity was about 6 dB below the AM intensity indicating that the PI approach was more effective at cancelling the linear signal components.

The CTR (Fig. 5b) represents the expected improvement in

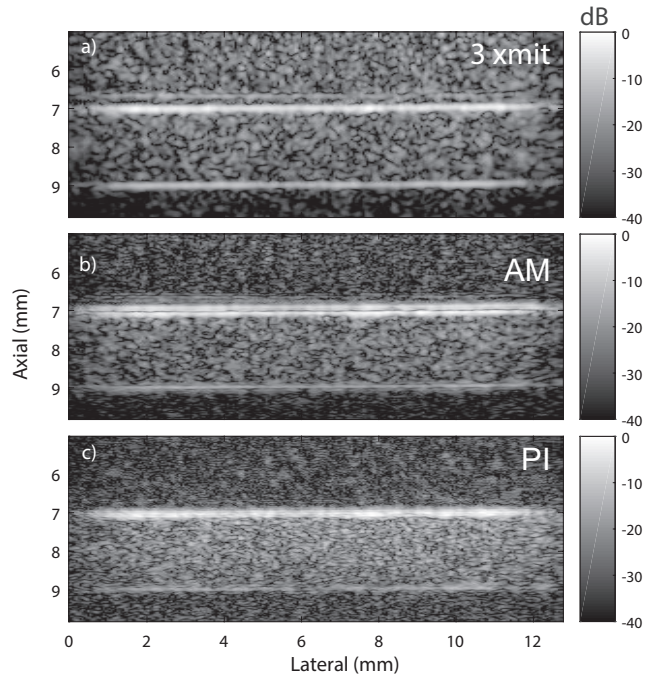


Fig. 4. Representative flow images for a 20 degree total angle span, 15 V (0.46 MPa derated) drive 1.5 cycle. a) normal multi-angle three transmissions, b) AM and c) PI. 0 dB is referenced to max intensity of each image.

contrast to localize *in vivo* contrast flow. The standard imaging case maintained a CTR of 3 dB across the drive pressures. The PI and AM cases showed an  $\approx 5\text{-}10$  dB enhancement of the flow region relative to background for derated pressures above 0.3 MPa. The ANOVA and Tukey test analysis of the three means revealed that the means of the PI and AM cases were statistically different from the 3-angle transmission case for acoustic drive pressures for derated pressures above 0.3 MPa ( $p < 10^{-4}$ ).

#### IV. CONCLUSIONS

The frequency response of the 18-MHz linear-array used in these studies did not allow for an ideal broadband frequency range that permitted a second harmonic or subharmonic to be readily detected. In addition, the AM transmit, while amplitude matched, had subtle phase changes that led to a greater residual than for the PI case. This means that while AM showed improvement in CTR relative to standard multi-angle plane-wave imaging, an improved waveform matching would further improve CTR relative to PI.

The results show that multi-pulse techniques can still be effective at high-frequencies even when the transducer is not ideal or when the transmit frequency is much higher than what the UCAs were designed for. Due to the wide size distribution, the backscattered signal has a rich harmonic and fundamental content throughout the bandwidth and it is not a requirement to filter and detect just the subharmonic or higher-harmonic content. Filtering in the bandwidth of the transducer still revealed nonlinear residuals in the AM and PI receive signals. Viti et al. [5] reached a similar conclusion using a 4.6

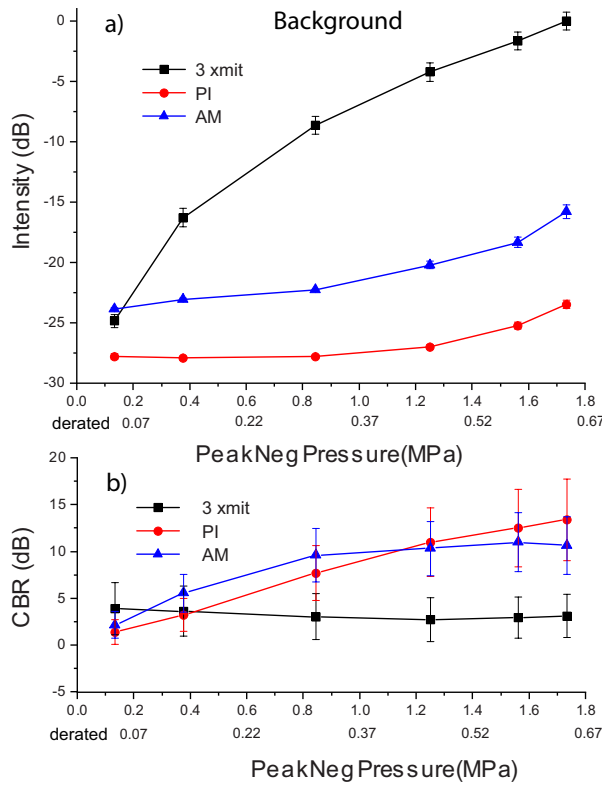


Fig. 5. Absolute RMS values from a) background and b) the CTR as drive pressure increased. The intensities of a) were greatest for the standard multi-angle plane-wave imaging case and the PI case had the lowest intensity. The AM and PI sequences enhanced the CTR by 5-10 dB relative to the standard multi-angle imaging sequence. The RMS intensity data (a) were normalized to the total number of transmissions (3 for standard multi-angle, 6 for PI and AM). The derated rated pressures accounting for attenuation in the phantom at an 8-mm depth are also shown on the x-scale bar.

MHz linear array with 104% bandwidth as have others [7], [14].

Our CTR values above a derated pressure of 0.3 MPa were between 8 and 13 dB with a relative change versus a 3-angle transmission case of between 5 and 10 dB. These results were very close to the 6 dB relative improvement Kusunose and Caskey [7] observed for PI also using an in-house UCA, plane-waves and a Verasonics system but at 2 MHz. Needles et al. [15] utilized a linear array with focused transmits using the UCA MicroMarker (FUJIFILM VisualSonics, Inc., Toronto, ON, Canada) and saw a CTR in the 18-MHz fundamental band of 12 dB with standard imaging, 15 dB with PI and 24 dB with AM, a 3 dB improvement for PI. The relative change in CTR between standard imaging and a multi-pulse approach helps normalize the results because phantoms and experimental parameters vary across reports in the literature. Although there are differences in exposure parameters, phantoms and measurement methods, the results reported here are consistent with past experimental work [5], [7], [15], [16].

#### V. ACKNOWLEDGEMENTS

This research was supported by grants from the National Institutes of Health (HD097485, EB022950, EY028550,

EY025215 and P30 EY019007), an Investigator Sponsored Trial grant from Lantheus Medical Imaging, Inc., and an unrestricted grant to the Dept. of Ophthalmology of Columbia U. from Research to Prevent Blindness.

#### REFERENCES

- [1] K. E. Morgan, J. A. Allen, P. A. Dayton, J. E. Chomas, A. L. Klibanov, and K. W. Ferrara, "Experimental and theoretical evaluation of microbubble behavior: Effect of transmitted phase and bubble size," *IEEE Trans. Ultrason. Ferroelect. Freq. Contr.*, vol. 47, pp. 1494-1509, 2000.
- [2] R. J. Eckersley, C. T. Chin, and P. N. Burns, "Optimising phase and amplitude modulation schemes for imaging microbubble contrast agents at low acoustic power," *Ultrasound Med. Biol.*, vol. 31, pp. 213-219, Feb. 2005.
- [3] D. H. Simpson, C. T. Chin, and P. N. Burns, "Pulse inversion Doppler: a new method for detecting nonlinear echoes from microbubble contrast agents," *IEEE Trans Ultrason Ferroelectr Freq Control*, vol. 46, pp. 372-382, 1999.
- [4] G. A. Brock-Fisher, M. D. Poland, and P. G. Rafter, "Means for increasing sensitivity in non-linear ultrasound imaging systems," US Patent 5,577,505A, Nov. 26, 1996.
- [5] J. Viti, H. J. Vos, N. d. Jong, F. Guidi, and P. Tortoli, "Detection of contrast agents: Plane wave versus focused transmission," *IEEE Trans Ultrason Ferroelectr Freq Control*, vol. 63, pp. 203-211, Feb. 2016.
- [6] O. Couture, S. Bannouf, G. Montaldo, J.-F. Aubry, M. Fink, and M. Tanter, "Ultrafast imaging of ultrasound contrast agents," *Ultrasound Med Biol*, vol. 35, no. 11, pp. 1908-1916, Nov 2009.
- [7] J. Kusunose and C. F. Caskey, "Fast, low-frequency plane-wave imaging for ultrasound contrast imaging," *Ultrasound Med. Biol.*, vol. 44, pp. 2131-2142, Oct. 2018.
- [8] D. E. Goertz, N. de Jong, and A. F. van der Steen, "Attenuation and size distribution measurements of Definity<sup>tm</sup> and manipulated Definity<sup>tm</sup> populations," *Ultrasound Med Biol*, vol. 33, pp. 1376-1388, 2007.
- [9] J. A. Ketterling, J. Mamou, J. S. Allen, O. Aristizabal, R. G. Williamson, and D. H. Turnbull, "Excitation of polymer-shelled contrast agents with high-frequency ultrasound," *J Acoust Soc Am-EL*, vol. 121, pp. EL48-EL53, 2007.
- [10] O. Aristizabal, J. Mamou, J. A. Ketterling, and D. H. Turnbull, "High-throughput, high-frequency 3D ultrasound for in utero analysis of embryonic mouse brain development," *Ultrasound Med. Biol.*, vol. 39, pp. 2321-2332, 2013.
- [11] B. Y. S. Yiu, I. K. H. Tsang, and A. C. H. Yu, "GPU-based beamformer: fast realization of plane wave compounding and synthetic aperture imaging," *IEEE Trans Ultrason Ferroelectr Freq Control*, vol. 58, no. 8, pp. 1698-1705, Aug 2011.
- [12] S. Stapleton, H. Goodman, Y.-Q. Zhou, E. Cherin, R. M. Henkelman, P. N. Burns, and F. S. Foster, "Acoustic and kinetic behaviour of Definity in mice exposed to high frequency ultrasound," *Ultrasound Med. Biol.*, vol. 35, pp. 296-307, Feb. 2009.
- [13] J. E. Browne, K. V. Ramnarine, A. J. Watson, and P. R. Hoskins, "Assessment of the acoustic properties of common tissue-mimicking test phantoms," *Ultrasound Med. Biol.*, vol. 29, pp. 1053-1060, Jul. 2003.
- [14] C.-C. Shen and P.-C. Li, "Pulse-inversion-based fundamental imaging for contrast detection," *IEEE Trans. Ultrason. Ferroelect. Freq. Contr.*, vol. 50, pp. 1124-1133, Sep. 2003.
- [15] A. Needles, M. Arditi, N. G. Rognin, J. Mehi, T. Coulthard, C. Bilan-Tracey, E. Gaud, P. Frinking, D. Hirson, and F. S. Foster, "Nonlinear contrast imaging with an array-based micro-ultrasound system," *Ultrasound Med Biol*, vol. 36, no. 12, pp. 2097-2106, Dec 2010.
- [16] O. Couture, M. Fink, and M. Tanter, "Ultrasound contrast plane wave imaging," *IEEE Trans Ultrason Ferroelectr Freq Control*, vol. 59, pp. 2676-2683, Dec. 2012.